

Article

Analysis of Cable Screen Currents for Diagnostics Purposes

Krzysztof Lowczowski * , Zbigniew Nadolny and Bartosz Olejnik

Faculty of Electrical Engineering, Poznan University of Technology, 60-965 Poznań, Poland; zbigniew.nadolny@put.poznan.pl (Z.N.); bartosz.olejnik@put.poznan.pl (B.O.)

* Correspondence: krzysztof.lowczowski@put.poznan.pl; Tel.: +48-61-665-2270

Received: 11 February 2019; Accepted: 4 April 2019; Published: 8 April 2019



Abstract: This paper presents current flow in cable screens and a cable screen earthing system. Moreover, the paper presents the methodology for the detection of problems in cable screens, such as open phase in a cable screen and high contact resistance of a cable screen in a cable joint. This is based on cable screen current measurements and allows for localization of the erroneous connection—high contact resistance or open phase. The phenomenon is simulated in PowerFactory Software. Moreover, exemplary cable screen current measurements are presented.

Keywords: cable screen; diagnostics; contact resistance; capacitive current

1. Introduction

Current flow in cable screens is often presented in literature in the context of cable screen losses [1,2]. In order to reduce cable screen losses, different methods can be utilized, i.e., cross-bonding or single point bonding [3]. The effectiveness of loss reduction methods is based on an assumption that cable screens are connected properly and the contact resistance of cable screens is negligible. Unfortunately, in some cases, cable screens could be connected incorrectly, which leads to extensive heating and changes the current flow in cable screens. Some publications report a big difference between simulation results and measurements, e.g., an error in the CB (cross bonded) line is in range of tens of percent [4]. Before the configuration of a cable screen is changed, one has to measure and analyze the current flow in the cable screen to make sure that losses will be reduced as planned and to make sure that cable screen connections are made correctly. If the cable screen is not connected properly, the effectiveness of loss reduction methods would be compromised. In a worst case scenario, a fragment of a cable screen could be left without earthing if single point bonding would be applied in a cable with a broken cable screen. In the case of single point grounding transient overvoltage, a cable screen during earth faults would be in the range of 10–15 kV, and therefore sheath voltage limiters would be recommended [5,6].

Cable lines are built according to the state of the art, which ensures high quality of cable installation [7,8]. It is, however, noted that there is no international standard regarding cable screen connections. Literature presents general information about contact resistance, e.g., about contact resistance of electromagnetic relays [9,10], but information about cable screen resistance is limited to a few publications, e.g., [11]. Problems with cable screen connection exist due to a lack of standards, bad design, non-clear installation procedures, unskilled personnel, and a lack of information about the installation of power cables. The lack of information is a particularly big problem in the case of watertight cables, which consist of double screen layers, since different manufacturers have different recommendations regarding double screen earthing and taking into account second screen layer conductivity in cable specification [12]. The problematic state of cable screen connections is

currently being analyzed by CIRED Working Group—Ground Screen Power Cable Connections—Test Recommendations for Ground Screen Power Cable Connections.

One has to realize that some damages result from mechanical damages and cannot be avoided, whereas some damages result from aging or operational errors [13]. Diagnostics of cable sheath damages is performed by means of direct current (DC) sources [14], whereas the diagnosis of cable screen connections is made by means of resistance meters. Diagnostics methods require a lot of work and therefore are seldom used in extensive medium voltage (MV) cable networks. In order to diagnose cable screen connections, it is possible to monitor cable screen currents. It is noted that information about the utilization of cable screen currents for diagnostics purposes is limited [15].

This paper presents a methodology for the identification and the localization of erroneous cable screen connections in two-point bonded MV cables, which are commonly used in Poland. The presented methodology is simple and allows for achieving full efficiency of cable screen loss reduction. Moreover, a risk of cable failure due to excessive heating or increased overvoltage in cable screen is reduced.

Current and voltage waveforms measured in cable screens can also be used for earth fault detection or for fault localization in alternating current (AC) or DC systems [16–19]. Analysis of cable screen currents gives a possibility to distinguish the type of line (cable or overhead) affected by an earth fault [20]. Furthermore, cable screen current measurements can be used for the detection of problems in cross bonded lines, e.g., short-circuited cable screens during flooding or insulation breakdown in cable joints [21–23]. Furthermore, the wrong order of cable screen connections in parallel connected cables can be detected.

2. Problem Formulation

This paragraph presents the theoretical background, which is necessary to interpret measurement and simulation results.

Figure 1 presents factors affecting current flow in cables screens and earth currents in cable screens under load conditions. Current flow in a cable screen is a result of inductive and capacitive coupling between cable cores and cable screens. Capacitive coupling is a source of screen and earth currents under no-load conditions and load conditions. Inductive coupling is a major source of current under load conditions.

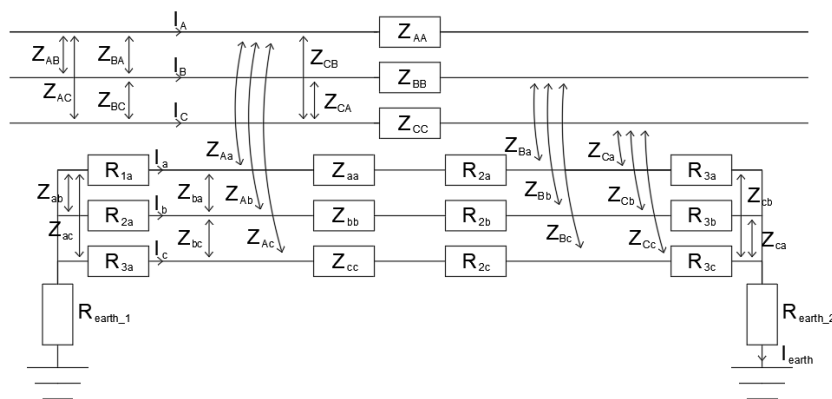


Figure 1. Factors affecting screen current flow under load conditions, where: Z —impedance, R —resistance, A, B, C —cable cores, a, b, c —cable screens, 1—cable beginning, 2—cable joint, 3—cable end.

Current flowing through cable cores—load current is a source of current in cable screens. In the case of single core cables in a three phase European system, each cable core is coupled with three cable screens, e.g., a current flowing through a cable core of phase A is a source of current flowing through a screen of the same cable—marked as (a) due to inductive coupling Z_{Aa} . The same core current is

also the source of currents in cable screens (b) and (c) because of inductive coupling Z_{Ab} and Z_{Ac} . Similar coupling exists between other phases, which are presented in Figure 1. As a result of inductive coupling, relatively high current flows through cable screens. An amplitude of the screen currents depends on cable type, cable formation, and load current. If the load current is symmetrical and the cables are laid in a trefoil formation (Figure 2c), screen currents are also symmetrical. In some cases, a cable laid in a trefoil formation could change the formation—a middle cable could collapse, and a flat formation could be formed (Figure 2b). Coupling impedances between cable cores and screens in flat formations differ significantly, and the screening effect between cables is weakened. As a result, the currents flowing through the cable screens rise and become unbalanced (asymmetrical); the current amplitude in the cable screen of the middle cable is lower even under balanced load conditions.

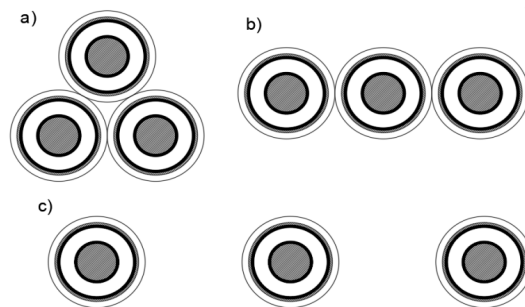


Figure 2. Cable formations: (a) trefoil, (b) flat, (c) flat, the distance between cables equal to one cable diameter (analyzed cable presented in right proportions).

Figure 3 presents an amplitude of the capacitive current flowing in a cable screen under no-load conditions. As can be observed, under no-load conditions, the currents flow from both cable ends to the middle of the cable line. In an ideal case (marked in blue), the current amplitude decreases linearly from both cable ends until it reaches half of the cable length. In the middle of the cable, the current amplitude is zero. It is assumed that the current measured at the cable ends in the ideal case is 1 pu (100%). In the case of the erroneous connection in a cable screen, the current flow under no-load conditions is changed significantly. If a distance between the supplying station and the open-phase is within 25% of a cable length, a screen current amplitude measured at the supply side drops to the level 0.5 pu (50%) and decreases from the supply side until it reaches 25% of the cable length. Afterwards, the screen current amplitude rises from 0 to 1.5 pu (150%) at the cable end (marked in orange). The sum of the currents measured at both cable ends is always 2 pu. Similar reasoning can be carried out to describe the screen current flow in a cable with the open-phase connection in 80% of the cable length (marked in red).

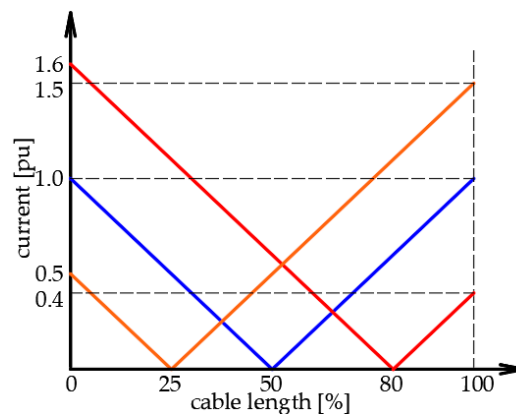


Figure 3. Cable screen current under no-load conditions as a function of cable length; orange represents open-phase in cable screen in 25% of cable length, blue represents ideal cable, and red represents open-phase in cable screen in 80% of cable length.

Under no-load conditions, the earth current— I_{earth} flow is a result of a voltage difference between both cables ends. In the case of proper connections, voltages induced by capacitive coupling in three screens neglect each other; however, when an erroneous connection exists in a cable screen, a resultant voltage is induced. The resultant voltage can be observed only when a cable is a single point bonded. According to simulation results under no-load conditions, an earth current depends mostly on an erroneous resistance. Therefore, simplified formulas describing earth current flow under no-load conditions can be used. Cable capacitance and conductance, which are sources of voltage in cable screens under no-load conditions, are described by formulas:

$$C_i = \frac{2\pi\epsilon_0 \cdot \epsilon_r}{\ln(r/q)} \quad (1)$$

$$G_i = \omega C_i \cdot tg(\delta) \quad (2)$$

where ϵ_0 —vacuum permittivity, ϵ_r —relative permittivity of the insulating layer, r is the outside radius of the insulation, q is the inside radius of the insulation, and $tg(\delta)$ —dielectric loss factor of the insulating layer.

Voltages induced in cable screens under no-load conditions are described by:

$$U_{healthy_SS} = U_{healthy_LS} = I_{healthy_LS} / \frac{1}{2} (G_i + j\omega C_i) \quad (3)$$

$$U_{erroneous_SS} = I_{erroneous_SS} / l_{distance} (G_i + j\omega C_i) \quad (4)$$

$$U_{erroneous_LS} = I_{erroneous_SS} / (100 - l_{distance}) (G_i + j\omega C_i) \quad (5)$$

Finally, voltages at cable ends are described by formulas:

$$U_{SS} = U_{healthy_SS} + U_{erroneous_SS} \quad (6)$$

$$U_{LS} = U_{healthy_LS} + U_{erroneous_LS} \quad (7)$$

Earth current is obtained after calculating:

$$U_{SS} - U_{LS} = I_{earth} (R_{earth_1} + R_{earth_2} + R_{soil} + R_{parallel_screens}) \quad (8)$$

where $U_{healthy_SS}$ —voltage at the supply side resulting from capacitive coupling between the cable core and the cable screen, U_{a,b,c_LS} —voltage at the load side resulting from capacitive coupling between the cable core and the erroneous cable screen, and $l_{distance}$ —a relative distance between the supply side and the erroneous connection, i.e., 20%.

When the cable line is installed properly, an earth current under no-load conditions is negligibly small. If the earth current under no-load conditions is in the range of decimal points, one can suspect that an erroneous connection is responsible for the increased amplitude.

When a cable line supplies a load, an amplitude of the earth current can be significantly higher because of the additional source—inductive coupling between cable cores and cable screens. A cable screen current is a function of load current. When the load current increases, the screen current increases as well. Relations between the cable core and the cable screen currents are presented in the literature, but an earth current is neglected. For cables laid in a trefoil formation, coupling impedances are approximately the same, and therefore the current flowing through cable screens is the same. As a result, the algebraic sum of currents is zero, and the earth current amplitude is also zero. In a trefoil formation, the earth current can be observed only during an earth fault. It must be emphasized that the earth current does not flow under an unbalanced load since the geometrical sum of currents is zero. The earth current flowing through the cable screen earthing system under the phase to earth fault conditions is a part of the zero sequence current.

The self-impedance of a conducting layer is given by the formula:

$$Z_{ii} = R'_i + \omega \frac{\mu_0}{8} + j\omega \frac{\mu_0}{2\pi} \ln \frac{D_e}{e^{-\frac{a\mu_r}{4}} \cdot r_i} \quad (9)$$

The mutual impedance is given by the formula:

$$Z_{ij} = \omega \frac{\mu_0}{8} + j\omega \frac{\mu_0}{2\pi} \ln \frac{D_e}{d_{ij}} \quad (10)$$

where R'_i —resistance per length of the conductor, ω —angular frequency ($2\pi f$), $\mu_0 = 4\pi \times 10^{-7}$ H/m, μ_r —relative permeability of the conductor material, r_i —radius of the conductor (m), d_{ij} —distance between the conductors (m), D_e —equivalent earth penetration depth (m), i, j —phase indices: A, B, C, a, b, c (Figure 1)

$$D_e = 658 \sqrt{\frac{\rho}{f}} \quad (11)$$

where ρ —earth resistivity (Ωm).

When the round conductor parameter $a = 1$, the case of the hollow conductor, a , is calculated according to the formula:

$$a = \left(1 - 4k^2 + (3 - \ln(k)) \cdot k^4\right) \cdot (1 - k^2)^{-2} \quad (12)$$

where k —the ratio of the inner and the outer conductor radiuses.

Self and mutual impedances between cores and screens are presented in the matrix form:

$$\begin{bmatrix} U_A \\ U_B \\ U_C \\ U_a \\ U_b \\ U_c \end{bmatrix} = \begin{bmatrix} Z_{AA} & Z_{AB} & Z_{AC} & Z_{Aa} & Z_{Ab} & Z_{Ac} \\ Z_{BA} & Z_{BB} & Z_{BC} & Z_{Ba} & Z_{Bb} & Z_{Bc} \\ Z_{CA} & Z_{CB} & Z_{CC} & Z_{Ca} & Z_{Cb} & Z_{Cc} \\ Z_{aA} & Z_{aB} & Z_{aC} & Z_{aa} & Z_{ab} & Z_{ac} \\ Z_{bA} & Z_{bB} & Z_{bC} & Z_{ba} & Z_{bb} & Z_{bc} \\ Z_{cA} & Z_{cB} & Z_{cC} & Z_{ca} & Z_{cb} & Z_{cc} \end{bmatrix} \cdot \begin{bmatrix} I_A \\ I_B \\ I_C \\ I_a \\ I_b \\ I_c \end{bmatrix} \quad (13)$$

In order to consider an erroneous connection, one has to change the real component of the cable screen self-impedance. To achieve the same result, it is also possible to divide an analyzed cable into two sections and add resistance between the sections.

Impedances in PowerFactory software are calculated based on geometrical parameters of the cable and the material parameters. The PowerFactory support lumped and distributed the parameters cable model. Considering the presented steady-state phenomenon, it is possible to use a simpler, lumped parameter model. In order to present the method of cable parameters calculation, an example of core self-impedance calculation is given. Core self-impedance is calculated according to formula (14):

$$Z_{cc} = Z_{11} + 2Z_{12} + Z_{22} \quad (14)$$

where impedances Z_{11} , Z_{12} , and Z_{22} are described by formulas (15), (16), and (17):

$$Z_{11} = Z_{c,out} + Z_{c/s,ins} + Z_{s,in} \quad (15)$$

$$Z_{12} = Z_{21} = Z_{s,mutual} \quad (16)$$

$$Z_{22} = Z_{s,out} \quad (17)$$

The impedances $Z_{c,out}$ and $Z_{s,in}$, and $Z_{s,mutual}$ are found with the modified Bessel functions [24]. Impedance $Z_{c/s ins}$ stands for the longitudinal voltage drop due to the magnetic field in the insulating layers and is given by formula (18):

$$Z_{ins} = j\omega \frac{\mu_0}{2\pi} \ln\left(\frac{q}{r}\right) \quad (18)$$

where r, q —outer, inner radius of the insulating layer.

The description of the advanced cable model for transient analysis can be found in [25]. Another model that includes ground return wire is presented in [26].

An erroneous connection in a cable screen connection reduces the screen current amplitude, as is required by Ohm law. Currents in other screens are higher than the current in the cable with an erroneous connection, and the algebraic sum of currents is greater than zero. As a result, the earth current is induced. When load current increases, the earth current increases as well since the algebraic sum is bigger. However, it must be emphasized that, in the case of a flat formation, an earthing current is present due to the asymmetry of the coupling impedances. The higher the asymmetry (distance between cables) is, the higher the earth current is induced.

Three single cores cables earthed at both ends (two points bonded) can be compared to three current transformers (CT) utilized in a residual connection (Holmgreen system), which are presented in Figure 4. The earth current can be compared with the zero-sequence current ($3I_0$) in the residual connection configuration. If phase or amplitude errors of current transformers utilized in the Holmgreen system are different, the geometric sum of the currents is greater than zero, and the zero sequence current is [27]. The earth current in single core cables is also induced when the load characteristic (dependency) of cables are different.

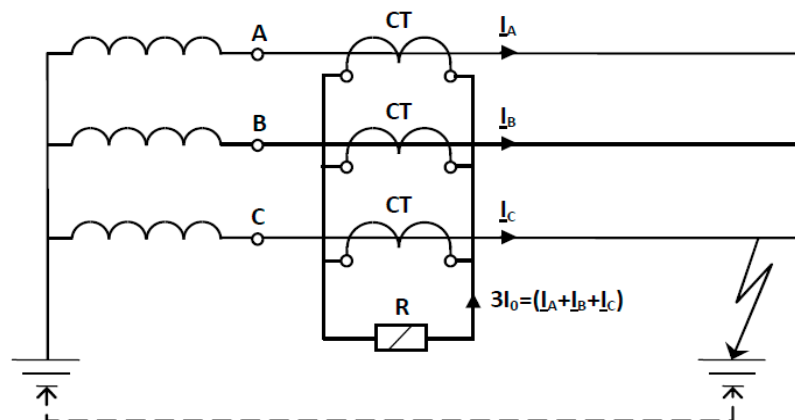


Figure 4. The principle of residual (Holmgreen) CT connection (CTs—line current transformers) [28].

3. Results

This section presents the measurement and the simulation results. Simulation software provides reference values, which are compared with measured values. The comparison shows clear deviations between the simulation and the measurement results. In order to analyze the case, sensitivity analysis is made with the help of simulation software.

3.1. Data Preparation

Measurements are taken in a 110/15 kV station, the general configuration of which is presented in Figure 5. The analyzed cable is the XRUHAKXS 3x120/50. According to the catalogue data, the XLPE insulation is 5.5 mm, the sheath is 2.5 mm, and the overall diameter is 35.8 mm. Radiuses of the cable core and the cable screen are calculated according to the formula describing the surface of the circle. Finally, a filling factor, which accounts for the compacting ratio, is adjusted, thus the resistances of the model are the same as the resistances specified in the catalogue. The cable supplies a traction

load, which explains the high variability of the load [29]. The first measurements are taken with clamp meters (Brymen BM135s) and a power quality analyzer (Fluke 435). The currents flowing through the cable screens are measured with clamp meters, which are equipped with a logger. The logger is able to store one minimum and one maximum current amplitude registered during the one minute period. The load current is measured with the Fluke 435, which is configured to save maximum and minimum current amplitudes every three seconds. In order to correlate the current flowing through the cable cores (load current) with the currents flowing through the cable screens, the recorded values are synchronized (time offset between measurements from different meters is removed) and resampled. Measurements taken by the Fluke are downsampled and, as a result, the maximal true RMS in phases A, B, and C for every minute is obtained. The processed measured cable screen currents are then compared with the reference values. The reference values can be obtained via simulation software, e.g., ATP, PSCAD, PowerFactory, or other simulation software. The procedure of obtaining the reference values in PowerFactory is presented in [1]. It is also possible to calculate the reference values by means of the formulas given in IEC 60287. The procedure can be performed with minimum values or average values if values are recorded. When professional meters with global positioning system (GPS) synchronization and high sampling rate are used, it is not necessary to perform the procedure described above.

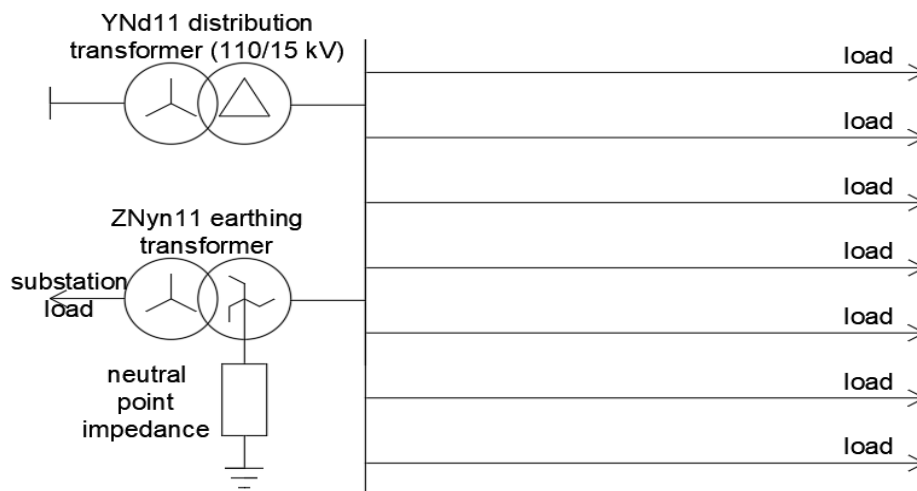


Figure 5. Typical distribution system network in Poland.

Figure 6 presents the current flowing through the cable cores in phases a, b, and c during the measurements. The corresponding measured screen currents are presented in Figure 7. As can be seen in Figure 6, the cable core currents (load currents) are symmetrical (the curves overlap each other), whereas the current flowing through the cable screens are asymmetrical—the amplitude of the cable screen current in phase B is significantly lower than those in phases A and C and is comparable with the amplitude of the earthing current. Additionally, the high earthing current during load conditions and the high asymmetry of the no-load current is noted.

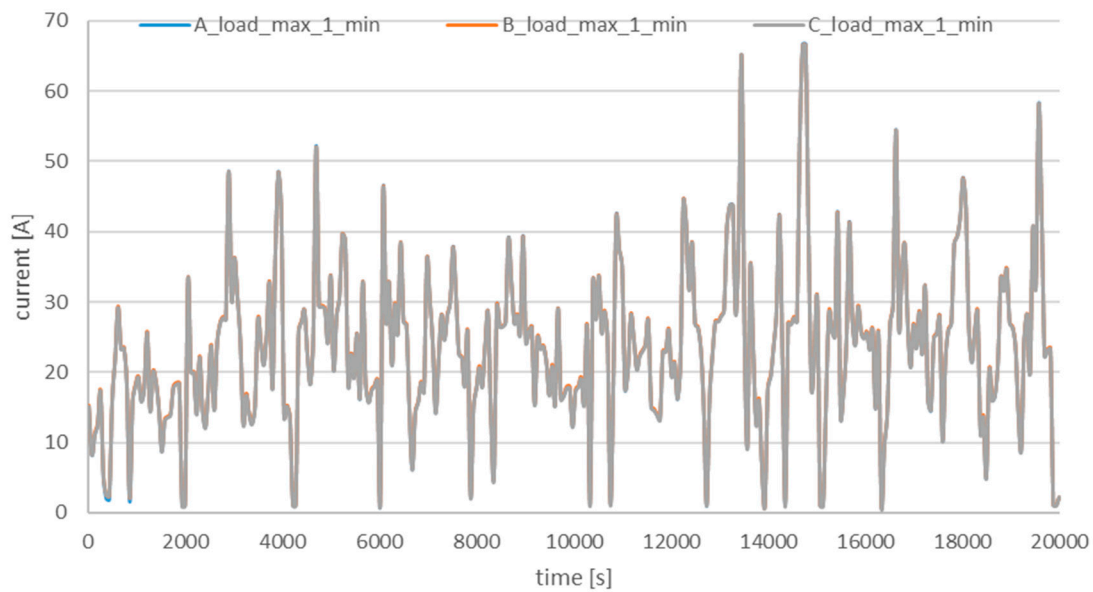


Figure 6. Measured load current (3 s measurements downsampled to maximum per 1 min).

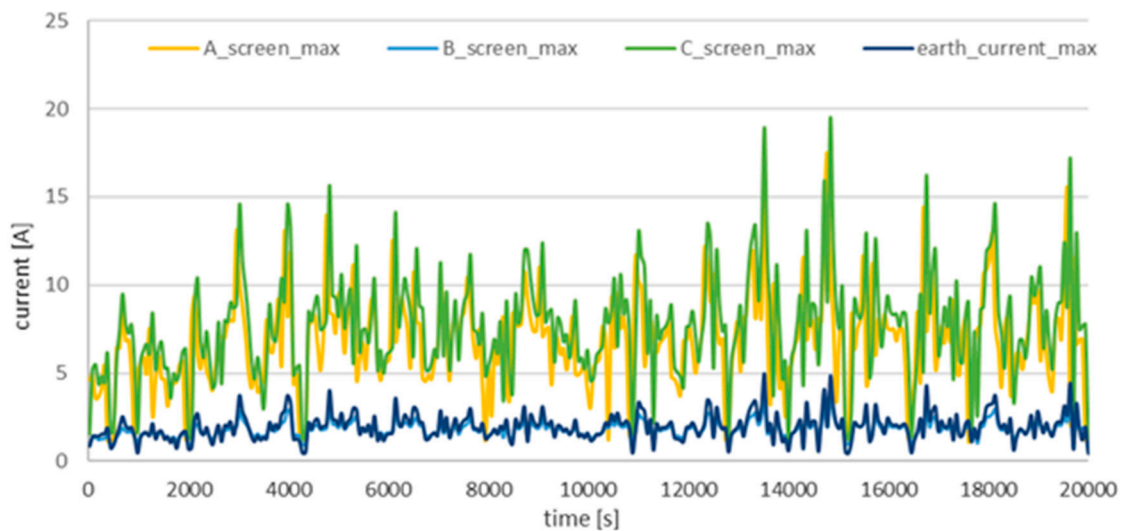


Figure 7. Measured cable screen current (max every 1 min).

Second measurements are taken on the cable screen with the Fluke 435 at the second end of the cable line. The measured cable screen currents are presented in Figure 8. The measurements allowed for the observation of the no-load current flowing from the load side. The no-load currents measured at both sides are given in Table 1. It can be observed that the current amplitude measured in two phases at both cable ends have almost the same amplitude, whereas the amplitude of the current measured in one phase is unusually low at the supply side and unusually high at the load side. Based on the unusually high unbalance (asymmetry) of the cable screen currents, an assumption can be made that additional resistance in one of the cable joints is responsible for the current flow. The cable is modeled and simulated in PowerFactory 2018 SP3 in order to verify the assumption.

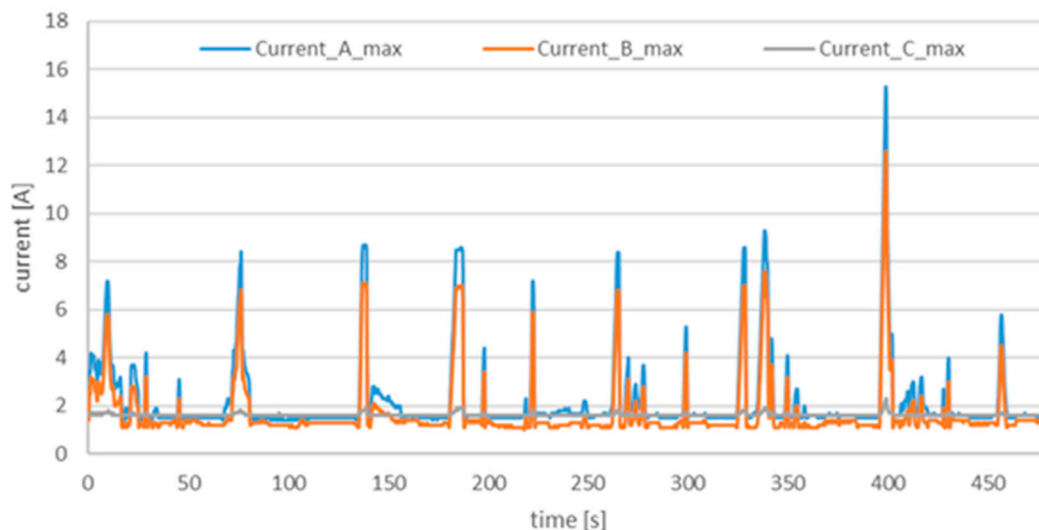
Table 1 presents exemplary screen currents for different cable formations. As can be observed, by increasing the distance between the cables, the amplitude of the screen currents and the screen currents' asymmetry increases as well. As a result, energy losses in the cable screens increase.

Table 1. Current flow in the cable cores and the screens.

| Load State | Cable Core (A) | | | Cable Screen (A) | | | Earthing System |
|--|--------------------|--------------------|--------------------|------------------|---------|---------|-----------------|
| | Phase A | Phase B | Phase C | Phase a | Phase b | Phase c | |
| Exemplary load state (110/15 kV substation; measured) | 35.7 | 35.7 | 35.5 | 9.89 | 2.33 | 11.18 | 3.05 |
| Reference for case A* (simulation results; 110/15 kV substation; formation: Figure 2a) | 35.7 | 35.7 | 35.5 | 5.4 | 5.35 | 5.5 | 0.73 |
| Reference for case B* (simulation results; 110/15 kV substation; formation: Figure 2b) | 35.7 | 35.7 | 35.5 | 7.13 | 4.27 | 8.28 | 0.73 |
| Reference for case C* (simulation results; 110/15 kV substation; formation: Figure 2c) | 35.7 | 35.7 | 35.5 | 10.19 | 7.82 | 11.64 | 0.75 |
| No-load conditions (110/15 kV substation; measured) | 2.5 | 2.6 | 2.8 | 1.32 | 0.92 | 1.31 | 0.36 |
| No-load conditions (MV substation; measured) | No-load conditions | No-load conditions | No-load conditions | 1.5 | 1.6 | 1.3 | 0.2 |

A*—XRUHAKXS cable laid in a trefoil formation (Figure 2a); B*—XRUHAKXS cable laid in a flat formation (Figure 2b); C*—XRUHAKXS cable laid in a flat formation with the distance between the cable equal to one diameter of cable (Figure 2c); MV—medium voltage.

One should note that the reference (simulated) currents have lower amplitudes because only the fundamental component is considered. The measurements taken by the author and other colleagues from the Institute of Electrical Engineering of Poznan University of Technology show clearly that the measured screen currents are typically 20-40% higher than the reference screen currents. In order to analyze the results properly, it is therefore better to compare the screen currents' unbalance or, if possible, to measure the fundamental component of the screen currents.

**Figure 8.** Measured cable screen current; sampling 0.25 s.

One can notice the difference between no-load currents measured at both cable ends. The no-load screen current depends on a few parameters, mostly voltage level and $\tan\delta$, which are used for diagnostics purposes. It is believed that registered differences result from different voltage levels during measurements. It is also believed that the no-load screen currents registered in reference to voltage level could be an indicator of insulation conditions.

3.2. Simulation Results

The model considers capacitive and inductive coupling. In order to analyze the impact of the contact resistance on the cable screen current flow, an automation script is developed [30]. The resistance and the location of an erroneous connection are changed in the loop. The erroneous connection is moved from the beginning to the end of the XRUHAKXS 3x120/50 cable line. The beginning and the end represent the terminals and the erroneous connection at the terminals, respectively, whereas the resistance along the cable line represents the joints and the erroneous connection at the cable joint. For each location of the erroneous connection, the resistance is changed from 1 to 20 Ω. The erroneous connection is in the middle cable, as presented in Figure 9. Simulation results are presented in Figures 10–13.

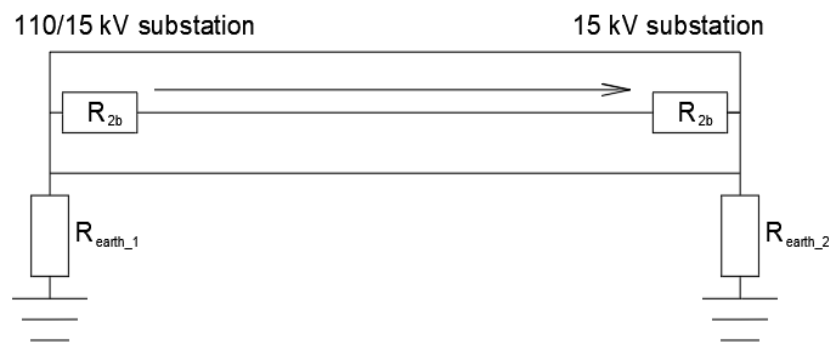


Figure 9. A schematic diagram of the simulations.

Unit impedance and admittance matrixes (Ω/km) of the analyzed cable are given below (A, B, C—cable cores; a, b, c—cable screens):

| | | | | | | |
|---------|--------------|--------------|--------------|--------------|--------------|--------------|
| | 1:R (A) | 2:R (B) | 3:R (C) | 4:R (a) | 5:R (b) | 6:R (c) |
| 1:R (A) | 3.02594e-01 | 4.92688e-02 | 4.92669e-02 | 4.92679e-02 | 4.92688e-02 | 4.92669e-02 |
| 1:X (A) | 7.41732e-01 | 6.37002e-01 | 6.38538e-01 | 6.92894e-01 | 6.37002e-01 | 6.38538e-01 |
| 2:R (B) | 4.92688e-02 | 3.02597e-01 | 4.92688e-02 | 4.92688e-02 | 4.92716e-02 | 4.92688e-02 |
| 2:X (B) | 6.37002e-01 | 7.41729e-01 | 6.37002e-01 | 6.37002e-01 | 6.92890e-01 | 6.37002e-01 |
| 3:R (C) | 4.92669e-02 | 4.92688e-02 | 3.02594e-01 | 4.92669e-02 | 4.92688e-02 | 4.92679e-02 |
| 3:X (C) | 6.38538e-01 | 6.37002e-01 | 7.41732e-01 | 6.38538e-01 | 6.37002e-01 | 6.92894e-01 |
| 4:R (a) | 4.92679e-02 | 4.92688e-02 | 4.92669e-02 | 4.03887e-01 | 4.92688e-02 | 4.92669e-02 |
| 4:X (a) | 6.92894e-01 | 6.37002e-01 | 6.38538e-01 | 6.92403e-01 | 6.37002e-01 | 6.38538e-01 |
| 5:R (b) | 4.92688e-02 | 4.92716e-02 | 4.92688e-02 | 4.92688e-02 | 4.03890e-01 | 4.92688e-02 |
| 5:X (b) | 6.37002e-01 | 6.92890e-01 | 6.37002e-01 | 6.37002e-01 | 6.92399e-01 | 6.37002e-01 |
| 6:R (c) | 4.92669e-02 | 4.92688e-02 | 4.92679e-02 | 4.92669e-02 | 4.92688e-02 | 4.03887e-01 |
| 6:X (c) | 6.38538e-01 | 6.37002e-01 | 6.92894e-01 | 6.38538e-01 | 6.37002e-01 | 6.92403e-01 |
| | 1:G (A) | 2:G (B) | 3:G (C) | 4:G (a) | 5:G (b) | 6:G (c) |
| 1:G (A) | 0.00000e+00 | 0.00000e+00 | 0.00000e+00 | -0.00000e+00 | 0.00000e+00 | 0.00000e+00 |
| 1:B (A) | 6.71818e+01 | 0.00000e+00 | 0.00000e+00 | -6.71818e+01 | 0.00000e+00 | 0.00000e+00 |
| 2:G (B) | 0.00000e+00 | 0.00000e+00 | 0.00000e+00 | 0.00000e+00 | -0.00000e+00 | 0.00000e+00 |
| 2:B (B) | 0.00000e+00 | 6.71818e+01 | 0.00000e+00 | 0.00000e+00 | -6.71818e+01 | 0.00000e+00 |
| 3:G (C) | 0.00000e+00 | 0.00000e+00 | 0.00000e+00 | 0.00000e+00 | 0.00000e+00 | -0.00000e+00 |
| 3:B (C) | 0.00000e+00 | 0.00000e+00 | 6.71818e+01 | 0.00000e+00 | 0.00000e+00 | -6.71818e+01 |
| 4:G (a) | -0.00000e+00 | 0.00000e+00 | 0.00000e+00 | 0.00000e+00 | 0.00000e+00 | 0.00000e+00 |
| 4:B (a) | -6.71818e+01 | 0.00000e+00 | 0.00000e+00 | 3.36170e+02 | 0.00000e+00 | 0.00000e+00 |
| 5:G (b) | 0.00000e+00 | -0.00000e+00 | 0.00000e+00 | 0.00000e+00 | 0.00000e+00 | 0.00000e+00 |
| 5:B (b) | 0.00000e+00 | -6.71818e+01 | 0.00000e+00 | 0.00000e+00 | 3.36170e+02 | 0.00000e+00 |
| 6:G (c) | 0.00000e+00 | 0.00000e+00 | -0.00000e+00 | 0.00000e+00 | 0.00000e+00 | 0.00000e+00 |
| 6:B (c) | 0.00000e+00 | 0.00000e+00 | -6.71818e+01 | 0.00000e+00 | 0.00000e+00 | 3.36170e+02 |

Figure 10 presents the screen current amplitude in the cable in which there is an erroneous connection as a function of resistance (ax x) and length between the supplying power station and the location of the erroneous connection (ax y). The current amplitude is marked in colors, i.e., red is 25 A, and dark blue is 5 A.

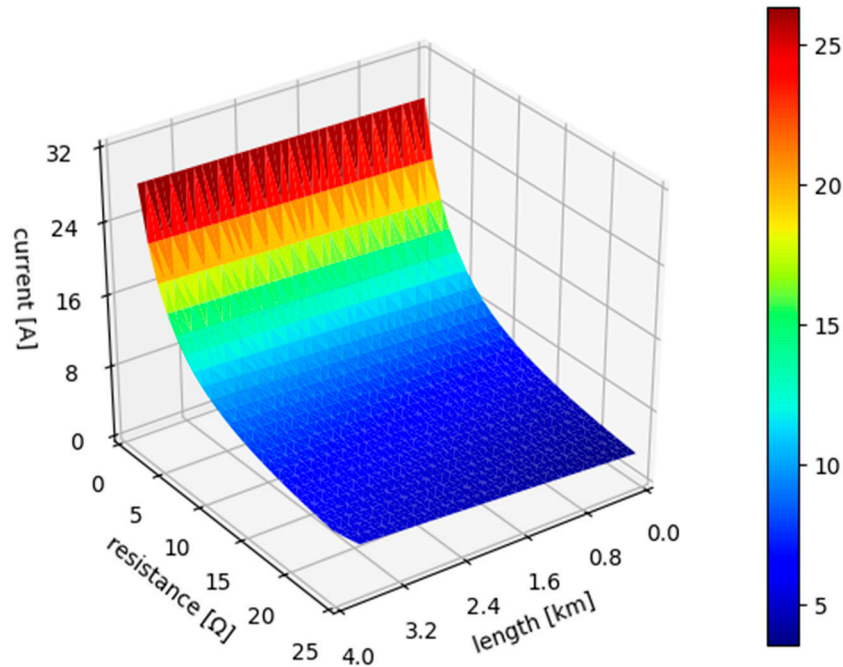


Figure 10. Current in the middle cable with additional resistance; formation presented in Figure 2c.

It is assumed that the cable is energized and supplies a 2.5 MW load. As can be observed, the amplitude of the screen current is strongly correlated with the resistance of the erroneous connection; the current drops when the resistance rises. It can also be observed that the location of the erroneous connection has a limited impact on the current amplitude. It is therefore difficult to localize the erroneous connection just by analyzing the cable screen currents under load conditions.

According to the simulation results, the earth current amplitude under no-load conditions is very similar for different cable formations, and therefore only the earth current for a flat formation is presented in Figure 11. It can be seen that the earth current measured at the supply side (110/15 kV station) has the lowest amplitude when the erroneous connection is in the middle of the cable line. Moreover, it can be seen that the earth current increases with the rise of resistance of the erroneous connection, and that earth current increases with the increasing distance between the erroneous connection and the middle of the line. The earth current under no-load conditions can be used for the identification of an erroneous connection in the cable screen. It is, however, difficult to specify the localization of the erroneous connection just by analyzing the earth current.

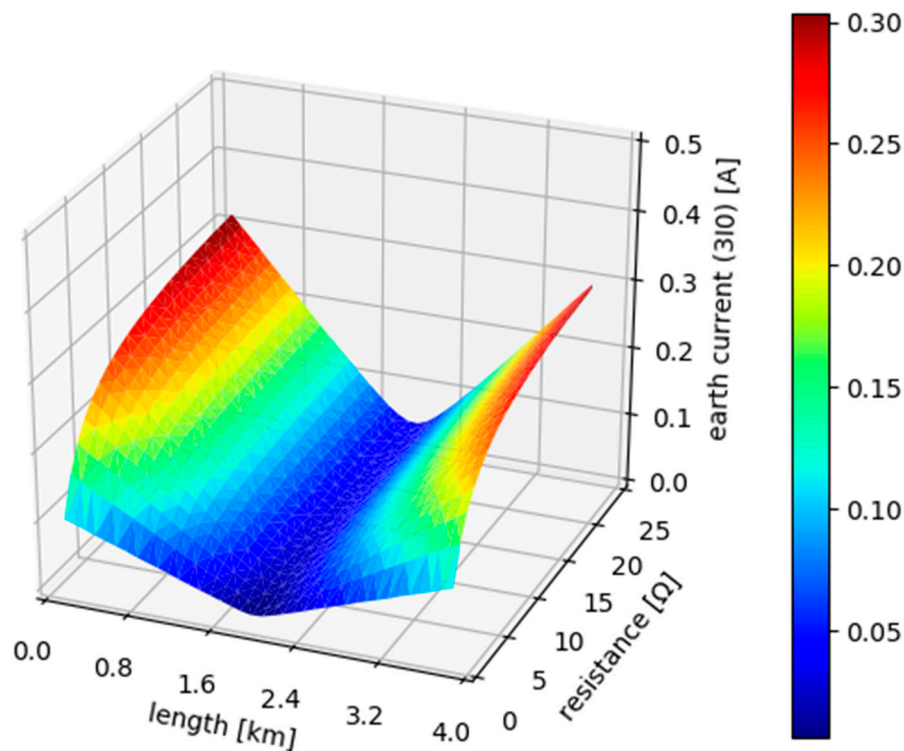


Figure 11. The earth current under no load conditions; formation presented in Figure 2c.

In order to localize the erroneous connection, amplitudes of the cable screen currents under no-load conditions should be analyzed. Figures 12 and 13 present the no-load screen current in a phase with an erroneous connection measured at both cable ends in a function of resistance and distance between the erroneous connection and supply side (cable beginning). As can be seen, the screen currents measured at both cable ends are inversely proportional; when the earth current measured at the supply station increases, the screen current measured at the load side decreases. Owing to the relationship between the two, it is possible to measure the screen currents at both cable ends and to calculate the distance between the cable ends and the erroneous connection. It is also possible to calculate the distance based on a single point measurement, however, if the second measurement point is included, the accuracy of the calculations is increased.

As can be seen in Figures 12 and 13, an impact of resistance on the current amplitude is limited, whereas the screen current amplitude strongly depends on the distance between the cable end and the erroneous connection. In many practical applications, it is possible to simplify analysis and consider only the distance between the erroneous connection and the cable end, as in the open-phase conditions presented in Figure 3. In order to calculate the approximate distance to an erroneous connection, one can use formula (14). Simplification is justified because faulty connections exist in cable joints, which are typically installed within a few hundred meters distance.

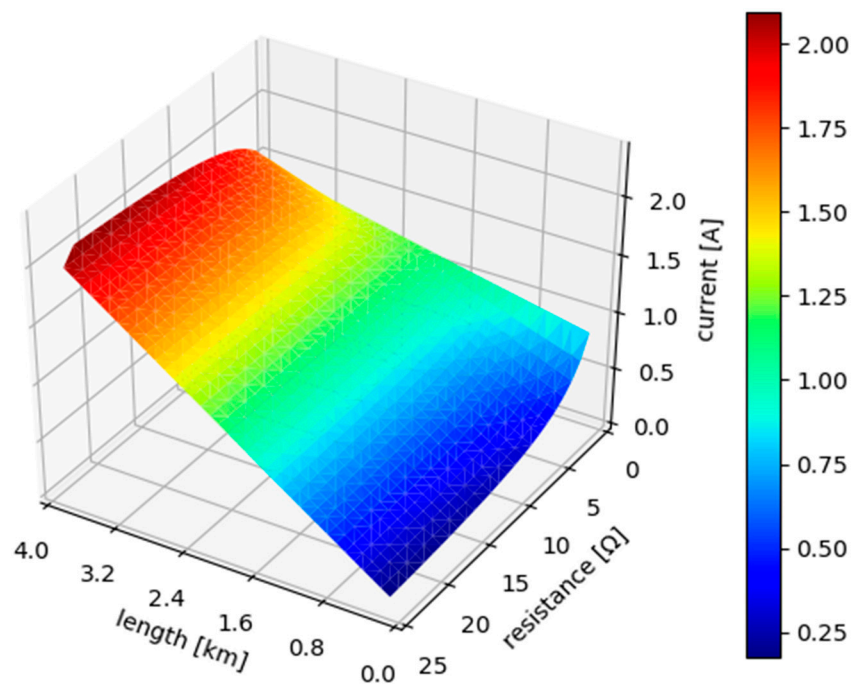


Figure 12. No-load screen current measured at the supply side; formation presented in Figure 2c.

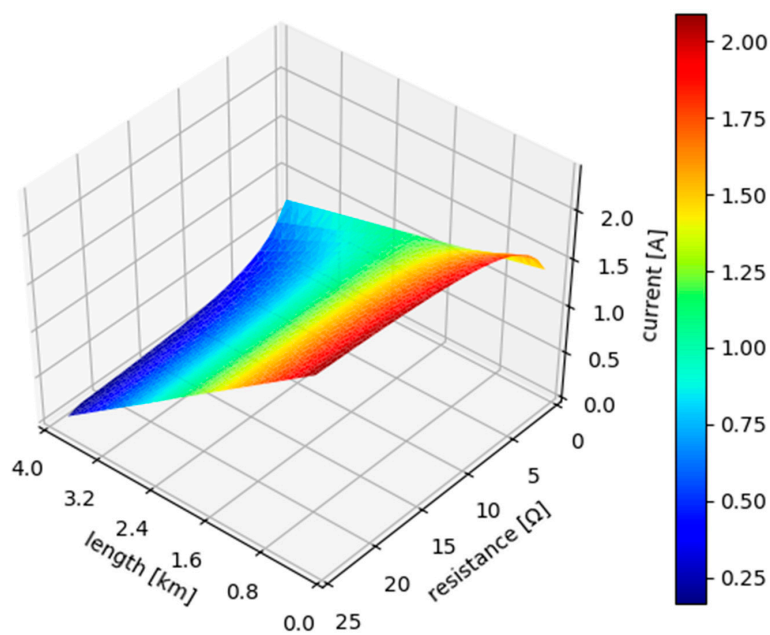


Figure 13. No-load screen current measured at the load side; formation presented in Figure 2c.

3.3. Proposed Methodology

Based on the presented analysis, the following procedure is proposed:

1. The measurement of cable screen currents on the energized cable.
2. If the amplitudes of the phase currents differ significantly, no-load screen currents should be measured.
3. If the no-load screen current in two phases is similar, one can assume that the connections in those phases are made properly and use the current as the reference.

4. The calculation of the distance to the erroneous connection. The formula is only valid for solid bonded cables.

$$L_{distance} = \frac{I_{erroneous_side} \cdot 0.5L_{cable}}{I_{ref}} \quad (19)$$

where $I_{erroneous_side}$ —no-load current measured at the supply side or the load side in the cable with the erroneous connection, $L_{distance}$ —distance between the supply side or the load side and the erroneous connection, e.g., 20%, I_{ref} —capacitive current in the properly made cable, L_{cable} —total cable length.

5. If the calculation indicates a location in which there are a few cable joints in close proximity, the screen current measurements should be repeated at the second end of the cable line.
6. The calculation of the reference current—an average of all “healthy” no-load screen currents.
7. The calculation of the distance to the erroneous connection.

If the cable length is unknown, one could use a repetitive pulse method to calculate the cable length [31]. The pulse diagnostic method is also recommended in a case of many erroneous connections along the cable line.

4. Discussion

This section presents factors that should be considered during the analysis of the cable screen currents flow.

Simple clamp meters are sufficient for the detection of abnormalities in cable screen connections under balanced load conditions. One should note that measurements have to be taken simultaneously in three phases. Clamps should be placed in an optimal position. Moreover, one has to pay attention to safety procedures. In some cases, an earth current could be increased because of harmonic distortions. Power quality analyzers offer additional possibilities, e.g., the observation of harmonics flow in the cable screen or the observation of the fundamental current. Moreover, power quality (PQ) meters take measurements synchronously, which minimizes the risk of erroneous measurements.

One should note that there are two types of clamp meters—RMS meters and true RMS meters. True RMS meters are considered better than RMS meters because power losses and heating effects can be calculated accurately. It is, however, difficult to compare true RMS screen currents with RMS references obtained from simulation software. In the case of cable screen current analysis, it is easier to use an old type RMS meter, which is equipped with a down-sample filter. Due to the filter, only the amplitude of the fundamental component is measured, and the comparison of references is simpler and more accurate [32]. If the load is unbalanced, advanced PQ meters have to be used.

In a typical high voltage (HV)/MV station, the resistance of the earthing system is approximately 0.1 Ω , whereas the grounding resistance in an MV/low voltage (LV) station in Poland is a few ohms, e.g., below 2.78 Ω [33]. As a result of the big difference between earthing resistances, it is possible that earthing current from different cables would flow through the first cable in the feeder. As a result, the measurement of the earthing current in a 110 kV station could be used for online monitoring of other cables in the feeder. Online monitoring would allow for early detection of abnormal screen connections. The presented methodology has limited sensitivity in the case of long feeders and therefore cannot fully replace conventional diagnostic methods, e.g., the measurement of the cable screen resistance. It should be considered as a complementary method that allows for simple, fast, and online measurement on an energized cable. Nevertheless, one has to consider safety procedures because during phase to ground or two phase to ground faults, the potential of cable screens could rise to dangerous levels.

The proposed method helps to improve the reliability of a power system. According to statistical data of some Polish distribution system operators, seven failures of cable lines per 100 km occur during a year [34]. High occurrences of failures and the increasing cost of non-supplied energy allow one to expect that the proposed method will be used in the future [35]. It is believed that in

the initial period, the proposed diagnostic method will help to increase the competence of workers, and in the next decade, the solution will be used for online control of cable screens of important cable lines [36]. The proposed method could be a part of an expert system, e.g., a fuzzy expert system that offers additional functionalities, e.g., localization of phase to ground faults or identification of failing components [37,38].

The presented methodology is limited to solid bonded cables. The authors plan to develop a methodology for the detection of an erroneous connection for other cable screen bonding methods. Moreover, it is planned to customize the methodology to HV cable lines.

5. Conclusions

Owing to the measurements, the problem of erroneous cable screen connections is noticed and discussed. Simulation software is used to find a source of unusually high screen current unbalance. Physical phenomena are explained, and general conclusions are made.

The erroneous connection of the two points bonded power cable can be identified via analysis of the cable screen currents. If unusually high asymmetry of currents flowing in the cable screen is observed, one can suspect there is a problem with the cable screen connections. To make sure that an erroneous connection is responsible for the current flow in the cable screens, it is recommended to measure the earthing current of the cable screens. If the earthing current is unusually high and depends on the load current, one can suspect an erroneous connection of the cable screen. If the cable line is installed properly, the earthing current under no-load conditions is negligibly small. After the erroneous connection is identified, one can pre-locate the erroneous connection. In order to assess the distance to the erroneous connection, amplitudes of the cable screen current under no-load conditions should be analyzed. Under no-load conditions, the current distribution in the cable screen with the erroneous connection is clearly affected; amplitudes of the screen currents flowing from both cable ends are different. In other phases with a proper connection, currents flowing from both cable ends have the same amplitude.

Simple clamp meters can be utilized for observing the current flow in cable screens when a load is symmetrical. However, it is recommended to use professional portable meters because the meters simplify the measuring process significantly and increase the accuracy of results, particularly when a load is unbalanced.

Author Contributions: K.L. software, B.O. validation, K.L., Z.N., B.O., formal analysis, K.L. investigation, Z.N. resources, K.L. data curation, K.L. writing—original draft preparation, K.L., Z.N. writing—review and editing, K.L. visualization, Z.N. supervision, Z.N. funding acquisition.

Funding: The research was financed from resources of the Ministry of Science and Higher Education for Statutory Activities No. 04/41/DS-PB/4347, name of the task: Improvement of Reliability of Supply in Distribution Network.

Conflicts of Interest: The authors declare no conflict of interest.

References

1. Lowczowski, K. Influence of power cable laying on cable sheath losses—Simulation in PowerFactory. *Prz. Elektrotech.* **2016**, *10*. [[CrossRef](#)]
2. Gouda, O.E.; Farag, A.A. Factors Affecting the Sheath Losses in Single-Core Underground Power Cables with Two-Points Bonding Method. *Int. J. Electr. Comput. Eng.* **2012**, *2*, 2088–8708. [[CrossRef](#)]
3. IEEE. *Guide for Bonding Shields and Sheaths of Single-Conductor Power Cables Rated 5 kV through 500 kV*; IEEE Standards Association: Piscataway, NJ, USA, 2014.
4. Chen, X.; Wu, K.; Cheng, Y.H. Sheath Circulating Current Calculations and Measurements of Underground Power Cables. In Proceedings of the JICABLE, Paris, France, 24–28 June 2007.
5. Heiss, A.; Balzer, G.; Schmitt, O.; Richter, B. Surge Arresters for Cable Sheath Preventing Power Losses in MV Networks. In Proceedings of the 16th International Conference and Exhibition on Electricity Distribution, Amsterdam, The Netherlands, 18–21 June 2001.

6. TRIDELTA Parafounders S.A. *HC Sheath Voltage Limiters*; TRIDELTA Parafounders S.A.: Bagnères-de-Bigorre, France, 2009; Available online: <http://destin.se/wp-content/uploads/2014/10/Destin-SA-cat-J-VARISIL-HC.pdf> (accessed on 5 February 2019).
7. Europacable. *Best Practice for the Installation of Medium Voltage Cable Accessories*; Europacable: Great Britain, UK, 2016.
8. CIGRE. *Large Cross-Sections and Composite Screens Design*; CIGRE: Paris, France, 2005.
9. Ksiazkiewicz, A.; Janiszewski, J. Low voltage relay contact resistance change influence by short-circuit current. *Ekspluat. Niezawod.* **2015**, *17*, 600–603. [[CrossRef](#)]
10. Liu, M. A New Method for Measuring Contact Resistance. In Proceedings of the XXVIIth General Assembly of the International Union of Radio Science, Maastricht, The Netherlands, 17–24 August 2002.
11. Yang, F.; Zhu, N.; Liu, G.; Ma, H.; Wei, X.; Hu, C.; Wang, Z.; Huang, J. A New Method for Determining the Connection Resistance of the Compression Connector in Cable Joint. *Energies* **2018**, *11*, 1667. [[CrossRef](#)]
12. Halvorson, H.L.; Hvidsten, S.; Kulbotten, H. Experiences with cable faults located at metallic screen connections. In Proceedings of the 24th International Conference & Exhibition on Electricity Distribution, Glasgow, Scotland, 12–15 June 2017.
13. SP Energy Networks. High Voltage Cable Strike with Excavator. Available online: https://www.spenergynetworks.co.uk/userfiles/file/mechanical_plant_hv_damages.pdf (accessed on 8 January 2019).
14. Megger. *MFM 10-1 Mobile, Battery Operated Sheath Fault Location System Up to ±10 kV DC*; Megger: Dover, UK, 2017.
15. Zhou, C.; Yang, Y.; Li, M.; Zhou, W. An Integrated Cable Condition Diagnosis and Fault Localization System via Sheath Current Monitoring. In Proceedings of the International Conference on Condition Monitoring and Diagnosis, Xi'an, China, 25–28 September 2016.
16. Aloui, T.; Amar, F.B.; Derbal, N.; Abdallah, H.H. Real time prelocalization of underground single-phase cable insulation failure by using the sheath behavior at fault point. *Electr. Power Syst. Res.* **2011**, *81*, 1936–1942. [[CrossRef](#)]
17. Jensen, C.; Nanayakkara, O.; Rajapakse, A.; Gudmundstottir, U.; Bak, C. Online fault location on AC cables in underground transmission systems using sheath currents. *Electr. Power Syst. Res.* **2014**, *115*, 74–79. [[CrossRef](#)]
18. Guo, F.; Zhu, G.; Dong, X. A Method of 20 kV Cable Line Fault Location Based on Sheath Grounding Current. In Proceedings of the IEEE Industry Applications Society Annual Meeting, Addison, TX, USA, 18–22 October 2015.
19. Arrabe, R.G.; Platero, C.A.; Gomez, F.A.; Lopez, E.R. New Differential Protection Method for Multiterminal HVDC Cable Networks. *Energies* **2018**, *11*, 3387. [[CrossRef](#)]
20. Arrabe, R.G.; Platero Gaona, C.A.; Gomez, F.A.; Lopez, E.R. Novel Auto-Reclosing Blocking Method for Combined Overhead-Cable Lines in Power Networks. *Energies* **2016**, *9*, 964. [[CrossRef](#)]
21. Dong, X.; Yang, Y.; Zhou, C.; Hepburn, D.M. Online Monitoring and Diagnosis of HV Cable Faults by Sheath System Currents. *IEEE Trans. Pow. Deliv.* **2017**, *32*, 2281–2290. [[CrossRef](#)]
22. Dong, X.; Yuan, Y.; Gao, Z.; Zhou, C.; Wallace, P.; Alkali, B.; Sheng, B.; Zhou, H. Analysis of Cable Failure Modes and Cable Joint Failure Detection via Sheath Circulating Current. In Proceedings of the Electrical Insulation Conference, Philadelphia, PA, USA, 8–11 June 2014.
23. Li, M.; Zhou, C.; Zhou, W.; Wang, C.; Yao, L.; Su, M.; Huang, X. A Novel Fault Location Method for a Cross-Bonded HV Cable System Based on Sheath Current Monitoring. *Sensors* **2018**, *18*, 3356. [[CrossRef](#)] [[PubMed](#)]
24. DigSILENT PowerFactory. Cable System. 2018. Available online: https://www.digsilent.de/en/powerfactory-download.html?folder=files%2Fdownloads%2Fprivate%2F10_PowerFactory%2F10_PowerFactory_2019%2F60_Technical+References#navigation7105 (accessed on 15 January 2019).
25. Hoshmeh, A.; Schmidt, U. A Full Frequency-Dependent Cable Model for the Calculation of Fast Transient. *Energies* **2017**, *10*, 1158. [[CrossRef](#)]
26. Angelov, J.; Vuletik, J.; Todorovski, M.; Ackovski, R. Equivalent circuit of single-core cable line with ground return wire and variable earth resistivity along its path. *Prz. Elektrotech.* **2014**, *90*, 100–104.
27. Schinerl, T. A New Sensitive Detection Algorithm for Low and High Impedance Earth Faults in Compensated MV Networks Based on the Admittance Method. In Proceedings of the 18th International Conference on Electricity Distribution, Turin, Italy, 6–9 June 2005.

28. Miedzinski, B.; Dzierzanowski, W.; Wisniewski, G.; Habrych, M. *Power System Protection*; Wroclaw, Poland, 2010. TFKable. Kable i Przewody Elektroenergetyczne. Available online: <https://www.tfkable.com/katalogi-i-broszury/katalogi.html> (accessed on 12 December 2018).
29. DigSILENT. PowerFactory 2018—Python Function Reference. 2018. Available online: https://www.digsilent.de/en/powerfactory-download.html?folder=files%2Fdownloads%2Fprivate%2F10_PowerFactory%2F10_PowerFactory_2019%2F60_Technical+References#navigation7105 (accessed on 15 January 2019).
30. Hernandez, S.E.; Acosta, L.; Toledo, J. Distance and Cable Length Measurement System. *Sensors* **2009**, *9*, 10190–10200. [[CrossRef](#)] [[PubMed](#)]
31. Lowczowski, K. Digital Protection Relays. Master's Thesis, Poznan University of Technology, Poznań, Poland, 2014.
32. Tauron Dystrybucja. *Standard techniczny nr 11/2015 budowy ukladow uzimowych w sieci dystrybucyjnej*; Technical standard nr 11/2015 Construction of Earthing System in Distribution Network; Tauron Dystrybucja: Krakow, Poland, 2017; Available online: <https://www.tauron-dystrybucja.pl/uslugi-dystrybucyjne/standardy-techniczne-sieci/ksiega-standardow-technicznych> (accessed on 14 December 2018).
33. Kornatka, M. Analysis of the exploitation failure rate in Polish MV networks. *Ekspluat. Niezawodn.* **2018**, *20*, 413–419. [[CrossRef](#)]
34. Paska, J. Chosen aspects of electric power system reliability optimization. *Ekspluat. Niezawodn.* **2013**, *15*, 202–208.
35. Antosz, K. Maintenance—Identification and analysis of the competency gap. *Ekspluat. Niezawodn.* **2018**, *20*, 484–494. [[CrossRef](#)]
36. Kaluder, S.; Fekete, K.; Jozsa, L.; Klaic, Z. Fault diagnosis and identification in the distribution network using the fuzzy expert system. *Ekspluat. Niezawodn.* **2018**, *20*, 621–629. [[CrossRef](#)]
37. Kulkarni, S.; Allen, A.; Lee, D.; Chopra, S.; Santoso, S.; Short, T. Waveform Characterization of Animal Contact, Tree Contact, and Lightning Induced Faults. In Proceedings of the IEEE PES General Meeting, Providence, RI, USA, 25–29 July 2010.
38. Kulkarni, S.; Allen, A.; Lee, D.; Chopra, S.; Santoso, S.; Short, T. Waveform Characteristics of Underground Cable Failures. In Proceedings of the IEEE PES General Meeting, Providence, RI, USA, 25–29 July 2010.



© 2019 by the authors. Licensee MDPI, Basel, Switzerland. This article is an open access article distributed under the terms and conditions of the Creative Commons Attribution (CC BY) license (<http://creativecommons.org/licenses/by/4.0/>).